M-2143

J. Chem. Thermodynamics **1987**, 19, 1305–1324

Thermodynamics of copper sulfides
III. Heat capacities and thermodynamic properties of $Cu_{1.75}S$, $Cu_{1.80}S$, and $Cu_{1.85}S$ from 5 to about 700 K

FREDRIK GRØNVOLD, SVEIN STØLEN,

Department of Chemistry, University of Oslo, Blindern, 0315 Oslo 3, Norway

EDGAR F. WESTRUM, JR., and CHARLES G. GALEAS

Department of Chemistry, University of Michigan, Ann Arbor, Michigan 48109, U.S.A.

(Received 23 March 1987; in final form 5 May 1987)

The heat capacities of $Cu_{1.75}S$, $Cu_{1.80}S$, and $Cu_{1.85}S$ have been measured by adiabatic-shield calorimetry from 5 to about 700 K. The heat-capacity curves show transitions near 312, 337, and 355 K in $Cu_{1.75}S$ and $Cu_{1.80}S$, and near 312, 368, and 376 K in $Cu_{1.85}S$, and occasion revision of existing phase diagrams. All transitions are characterized by hysteresis in the attainment of equilibrium and a greater or lesser dependence on thermal history and/or thermal recycling. Thermodynamic functions have been evaluated and selected values are, for $R = 8.3144\ J \cdot K^{-1} \cdot mol^{-1}$:

	$C^\circ_{p,m}/R$	$\Delta^T_0 S^\circ_m(T)/R$	$\Phi^\circ_m(T, 0)/R$	T/K
$(1/2.75)Cu_{1.75}S$	3.354	4.702	2.526	298.15
	3.571	8.104	4.977	700
$(1/2.80)Cu_{1.80}S$	3.614	4.708	2.527	298.15
	3.541	8.129	4.994	700
$(1/2.85)Cu_{1.85}S$	3.246	4.650	2.497	298.15
	3.476	8.085	4.945	700

1. Introduction

In (copper + sulfur) the region from Cu_2S to $Cu_{1.75}S$ shows a wide variety of phases and phase transitions at intermediate temperatures which need further elucidation from a thermodynamic point of view. The heat capacity and thermodynamic properties of synthetic chalcocite, Cu_2S, and synthetic covellite, CuS, have recently been redetermined.[1,2] In this paper similar determinations on $Cu_{1.75}S$, $Cu_{1.80}S$, and $Cu_{1.85}S$ are reported. The phases that occur have been characterized by X-ray diffraction and thermodynamic functions have been determined.

It has been recognized for a long time that the cubic high-temperature modification of Cu_2S, high-chalcocite or high-digenite, can contain excess sulfur to at least the composition $Cu_{1.80}S$. Buerger[3,4] presented evidence for $Cu_{1.80}S$ being

0021-9614/87/121305+20 $02.00/0

a separate phase (with pseudo-cubic structure) and revived the name digenite for the mineral. Electrochemical-cell studies by Wagner and Wagner[5] and by Wehefritz[6] in the region up to 720 K and sulfur decomposition-pressure studies by Rau,[7,8] by Nagamori,[9] and by Peronne *et al.*[10] in the region 680 to 1320 K have provided accurate information about the range of the high-digenite phase. Possible defect reactions were discussed. According to Rau[7] the composition limit of digenite is $Cu_{1.775}S$ at 351 K, whereas the homogeneity range extends from $Cu_{\approx 2.000}S$ to $Cu_{1.733}S$ at 780 K.

Donnay *et al.*[11] observed that diginite undergoes a rapidly reversible non-quenchable transition between 333 and 338 K and suggested the low-temperature form to be cubic with cell edge five times the face-centered high-digenite cell $\{a = 5a' = (2771 \pm 8)\ \text{pm}\}$ and with 100 Cu_9S_5 units per cell. The numerous absent reflections were interpreted in terms of a rhombohedral unit cell ($R\bar{3}m$, $a = 1616$ pm, $\alpha = 0.2432$) containing one Cu_9S_5 unit. Further single-crystal studies of synthetic digenite by Kullerud[12] and Morimoto and Kullerud[13] revealed that the rhombohedral form was metastable and reverted gradually with time to a stable low-temperature form. This form has cubic symmetry without the special extinction rules observed for the rhombohedral form.

According to Roseboom[14] low-digenite has a range of homogeneity from $Cu_{1.765}S$ to $Cu_{1.79}S$ at 300 K. The sulfur-rich composition limit is unobservably affected by temperature, while the copper-rich limit increases to $Cu_{1.83}S$ at 355 K where low-digenite transforms to high-digenite. Thus, digenite of composition $Cu_{1.80}S$ is unstable below 323 K according to Roseboom. When the composition changes in the vicinity of $Cu_{9-x}S_5$ the unit-cell parameter first increases continuously as x becomes smaller. Near Cu_9S_5 a discontinuous change of the super-cell length from 2780 to 3336 pm occurs, *i.e.* from five to six times the cell edge of high-digenite, respectively.[13] Electron-diffraction investigations[15–18] have revealed the existence of a series of related superstructures in low-digenite as function of temperature and composition, with spacings $2a$, $3a$, $4a$, $5a$, and $6a$. According to Pierce and Buseck[15] the ordered digenite and bornite phases consist of alternating cube-shaped vacancy-rich and copper-rich regions. Van Dyck *et al.*[16] argued that Cu atoms preferentially occupy complete (111) layers of tetrahedral interstices between close-packed planes in the face-centered cubic matrix of S atoms. Stacking of these planes gives rise to observed superstructures which need not be commensurate.

The phase relations in this region are even more complex since the discovery of a new low-temperature phase and mineral, anilite, with composition $Cu_{1.75}S$ by Morimoto *et al.*[19] The upper stability limit was given as (343 ± 3) K by Morimoto and Koto[20] and the orthorhombic structure was described in detail by Koto and Morimoto.[21] It contains five kinds of Cu atoms occurring in tetrahedral and triangular coordinations. The arrangement of the Cu atoms is ordered, and the concomitant displacement of S atoms results in a superstructure of the non-stoichiometric high-temperature form (high-digenite). While some later investigators expressed doubt as to the stability of anilite,[22–27] Potter[28] was able to confirm its stability by electrochemical studies. According to the phase diagram presented,

anilite ($Cu_{1.75}S$) decomposes into covellite (CuS) and digenite ($Cu_{1.765}S$) on heating to (348 ± 3) K, while digenite of composition $Cu_{1.805}S$ decomposes eutectoidally on cooling to (345 ± 3) K into anilite and another low-temperature phase (djurleite, $Cu_{\approx 1.95}S$), which will be considered in a forthcoming paper in this series. Gray[29] does not consider anilite as an independent phase, arguing that its structure is easily accounted for as a digenite structure with a rotation of the unit cell. However, as the different atoms do not take ideal cubic positions in the low-temperature structure such a consideration seems inappropriate.

At the outset of this work, Potter's results were not available to us, and the transition around 328 K for which we wanted to study the heat-capacity, was generally assumed to be from low- to high-digenite. In addition we wanted to study the formation of anilite and how anilite and djurleite influenced the extension of the digenite field. A gradual transition with maximum heat capacity around 350 K was found for $Cu_{1.80}S$, but the transitions in the range 300 to 340 K depended to some extent on previous history. Heat-capacity measurements at lower temperatures were, therefore, carried out on $Cu_{1.75}S$, $Cu_{1.80}S$, and $Cu_{1.85}S$. A transition around 312 K was found to be present in all three samples, as well as a small bump near 337 K for $Cu_{1.75}S$ and $Cu_{1.80}S$. The peak near 312 K was found to originate from a

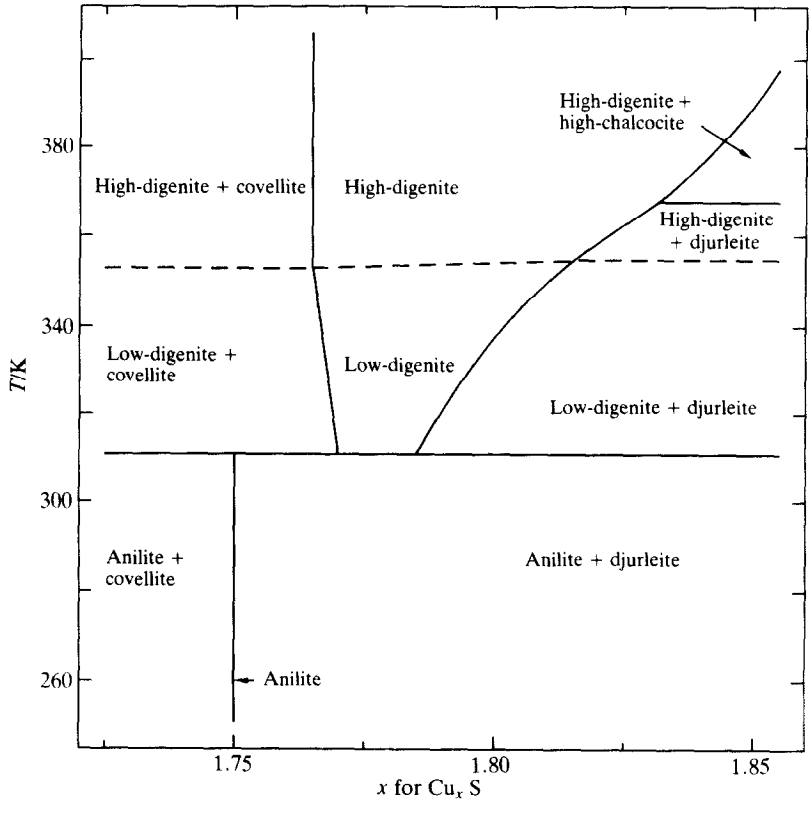

FIGURE 1. Part of the (copper + sulfur) phase diagram.

structural transition of the anilite phase ($Cu_{1.75}S$) to low-digenite,[30] while the hump near 337 K was ascribed to kinetically slow phase reactions. A modified phase diagram for this region is presented in figure 1. Previous observations by Luquet *et al.*[25] and Gezalov *et al.*[31] fit into this picture. Luquet *et al.*[25] reported a peak around 310 K in d.t.a. of $Cu_{1.765}S$ but did not comment on it further. Gezalov *et al.*[31] observed a transition between what they denoted as a pseudo-cubic orthorhombic lattice (presumably anilite) and low-digenite. According to Potter's phase diagram heating of truly equilibrated $Cu_{1.80}S$, consisting of anilite and djurleite, would however, result in eutectoidal formation of digenite at 328 K.

According to Gray and Clarke[32] two discrete equilibrium forms of digenite exist ($Cu_{1.89}S$ and $Cu_{1.84}S$). The room-temperature structures of the two digenites are described as three-dimensional N-fold commensurate superlattices such that the unit cell is a cube of side Na_0, with N equal to 10 and 12, respectively. This is not in accord with earlier interpretations, where these compositions are within the (anilite + djurleite) two-phase region.[28] At higher temperatures $Cu_{1.84}S$ and $Cu_{1.89}S$ transform into $5a_0$ and $6a_0$ superstructures, respectively.[32] According to Morimoto and Kullerud[13] the $5a_0$ superstructure is found for $x < 1.80$, whereas the $6a_0$ superstructure is found for higher values of x. This discrepancy may be ascribed to the calibration curve for determination of the compositions of the crystals used by Gray.[29] The calibration is based on the temperature dependence of the low- to high-digenite transition. However, the values shown in figure 2.4 in reference 29 (only three points in the region $1.70 < x < 1.97$) are not in accordance with the results of Roseboom[14] and in addition fail to show constant transition temperatures in the two-phase regions.

2. Experimental

The copper sulfides were prepared directly from the elements. The copper was in the form of a continuous cast rod, >99.999 mass per cent pure, from the American Smelting and Refining Co., New Jersey. The sulfur was 99.9999 mass per cent pure crystals from Koch-Light Laboratories Ltd., Colnbrook, England. Appropriate amounts of the elements were heated in an evacuated and sealed vitreous silica tube, constricted at the middle by a smaller-diameter tube. Copper was placed in one part of the tube and sulfur in the other, and the tube was put into a slightly inclined tube furnace with the sulfur-containing compartment protruding. The copper was heated to 620 K and the sulfur was allowed to melt and flow into the hotter part of the tube. After most of the sulfur had combined with the copper, a heating pad wound around the exterior end of the silica tube was used to bring the remaining sulfur into reaction overnight. The empty half of the silica tube was sealed off and discarded before the sample was tempered at 670 K for 24 h. The sample was then finally crushed and transferred to the calorimetric ampoule.

The characterization of the samples was done by powder X-ray diffraction, see below. The phases observed in the three samples, their lattice constants, and results of previous investigations are presented in table 1.

The calorimetry was as previously described,[1,2] the low-temperature (5 to

TABLE 1. Phases observed by X-ray powder diffraction at room temperature; the uncertainties represent one standard deviation

Composition x in Cu_xS	Phase	Unit-cell dimensions a/pm	b/pm	c/pm	Authors
1.75	Anilite	789.9 ±0.2	783.9 ±0.2	1101.4±0.3	Present
1.80	Anilite	789.7 ±0.2	783.8 ±0.2	1102.0±0.3	Present
	Djurleite	2692 ±1	1575 ±1	1356 ±1	Present[a]
1.85	Anilite	789.9 ±0.2	783.8 ±0.2	1101.5±0.3	Present
	Djurleite	2692 ±1	1575 ±1	1356 ±1	Present[a]
1.75	Anilite	790.65±0.08	782.23±0.08	1107.8±0.1	Potter and Evans[33]
1.75	Anilite	789 ±2	784 ±2	1101 ±2	Morimoto *et al.*[19]
1.934	Djurleite	2689.6 ±0.6	1569.4 ±0.3	1353.6±0.3	Potter and Evans[33][a]
1.96	Djurleite	2686 ±2	1570.0 ±0.6	1352.8±0.6	Djurle[34][a]
1.97	Djurleite	2692 ±5	1571 ±3	1356 ±3	Takeda *et al.*[35][a]

[a] Indexed according to an orthorhombic cell.

350 K) work having been done at the University of Michigan[36] and the high-temperature (300 to 700 K) work at the University of Oslo.[37]

The heat capacities of the empty calorimeters were determined in separate series of experiments. The heat capacity of the samples represented from about 95 to 80 per cent of the total in the low-temperature calorimeter and about 50 per cent in the high-temperature calorimeter.

Small corrections were applied for temperature excursions of the shields from the calorimeter temperature and for "zero drift" of the calorimeter temperature. Further small corrections were applied for differences in amounts of (indium + tin) solder, helium gas, and Apiezon-T grease for the low-temperature calorimeter and for differences in mass of the silica-glass containers for the high-temperature calorimeter. The masses of the sample used in both low- and high-temperature calorimeters were about 150 g.

Room temperature X-ray powder-diffraction photographs were taken in Guinier cameras of 80 mm diameter with Cu $K\alpha_1$ radiation, and Si as calibration substance, $a(293.15\ K) = 543.1065$ pm.[38]

High-temperature X-ray photographs were obtained between ≈ 290 and ≈ 700 K in an Enraf-Nonius (FR 553) Guinier-Simon camera (Cu $K\alpha_1$ radiation, quartz-crystal monochromator). The samples were contained in sealed thin-walled silica-glass capillaries. The temperature was regulated *via* a Pt resistance thermometer and a digital programmer, which synchronized the temperature increase with the movement of the film cassette. The difference between the programmed and actual temperature at the sample position is considered to be within 5 K. The experiments were done without internal standard to avoid uncontrolled reactions in the higher-temperature region. The Guinier-Simon camera factor was determined in terms of lattice constants obtained at 293 K by the Guinier-method.

Unit-cell dimensions were derived by applying the least-squares program CELLKANT.[39] Theoretical intensities of the reflections on the powder photographs were calculated by the program LAZY-PULVERIX.[40]

Differential-thermal-analysis (d.t.a.) measurements were performed with a Mettler

TABLE 2. Molar heat capacities of $Cu_{1.75}S$, $Cu_{1.80}S$, and $Cu_{1.85}S$ ($R = 8.3144\ J \cdot K^{-1} \cdot mol^{-1}$)

T/K	$C_{p,m}/R$	T/K	$C_{p,m}/R$	T/K	$C_{p,m}/R$	T/K	$C_{p,m}/R$	T/K	$C_{p,m}/R$	T/K	$C_{p,m}/R$

$M\{(1/2.75)Cu_{1.75}S\} = 52.099\ g \cdot mol^{-1}$

High-temperature measurements—University of Oslo

Series I		418.58	3.526	552.04	3.493	690.78	3.566	341.83	4.101	346.51	4.362
310.13	11.16	428.57	3.495	562.58	3.501	701.73	3.578	350.34	4.780	348.63	4.539
316.89	3.838	438.62	3.495	573.15	3.508	712.64	3.591	359.06	3.810	350.68	4.936
326.27	3.639	448.70	3.487	583.75	3.499	723.25	3.597	368.49	3.689	352.59	5.602
335.59	3.956	458.84	3.482	594.39	3.501	734.02	3.615	Series III		354.64	3.977
344.40	4.439	469.02	3.481	605.00	3.534	745.14	3.638	319.91	3.507	356.94	3.870
352.20	4.451	479.25	3.480	615.17	3.504	756.30	3.642	324.74	3.595	359.26	3.822
360.41	3.825	489.52	3.481	625.46	3.514	767.50	3.665	329.51	3.698	361.60	3.778
369.84	3.707	499.82	3.475	636.60	3.512	Series II		334.19	3.846	363.95	3.774
379.40	3.650	510.19	3.465	647.34	3.510	303.72	3.338	337.62	4.034	366.31	3.738
389.07	3.603	520.60	3.466	658.22	3.526	313.59	3.443	339.88	3.989	368.68	3.728
398.84	3.579	531.05	3.473	668.96	3.536	323.28	3.560	342.12	4.098	371.05	3.710
408.67	3.556	541.53	3.481	679.89	3.548	332.73	3.799	344.34	4.214	373.43	3.704

Low-temperature measurements—University of Michigan

Series IV		313.39	9.5754	Series IX		15.03	0.1535	299.37	3.3958	312.16	60.645
179.44	2.6920	325.24	3.8983	140.97	2.4221	16.42	0.1906	304.36	3.6819	312.31	47.965
184.15	2.7194	Series VI		150.89	2.5020	18.04	0.2378	307.71	4.4975	312.63	17.133
192.00	2.7635	300.80	3.4668	160.53	2.5731	19.71	0.2885	309.28	6.8550	313.76	4.1921
202.13	2.8139	313.94	9.0490	170.35	2.6386	21.59	0.3477	310.26	13.708	315.61	3.7582
211.34	2.8587	326.39	4.0040	180.19	2.6972	23.79	0.4183	310.78	25.521	317.53	3.8827
221.65	2.9094	Series VII		189.98	2.7534	26.20	0.4957	311.09	38.472	321.05	4.0281
231.80	2.9554	265.16	3.1150	Series X		28.84	0.5798	Series XIII		326.11	4.2033
241.81	3.0026	289.65	3.2643	92.82	1.8959	32.43	0.6900	228.44	2.9409	331.24	4.3178
251.70	3.0487	300.68	3.4683	102.50	2.0196	35.75	0.7880	278.56	3.1809	337.11	4.0838
261.68	3.0941	314.21	8.7862	111.94	2.1321	39.26	0.8852	293.51	3.2741	343.43	4.2572
271.74	3.1382	325.60	3.9205	121.80	2.2406	42.13	0.9589	299.42	3.3799	348.11	4.5123
281.48	3.1884	Series VIII		131.68	2.3392	45.69	1.0470	305.07	3.7246	Series XIV	
290.93	3.2568	53.28	1.2180	141.36	2.4256	50.19	1.1508	308.58	4.5902	296.46	3.3562
300.16	3.3701	58.34	1.3223	151.15	2.5040	54.75	1.2482	309.96	6.8674	302.99	3.4123
307.31	6.3364	63.41	1.4218	Series XI		Series XII		310.85	12.685	309.79	3.4769
311.22	33.728	69.02	1.5219	5.20	0.00505	141.89	2.3997	311.35	22.432	316.58	3.5525
316.61	3.8166	75.54	1.6313	6.00	0.00794	226.92	2.9348	311.65	35.784	325.31	3.6807
324.76	3.8006	82.60	1.7484	6.79	0.01167	270.57	3.1295	311.83	70.017	334.81	3.9161
Series V		90.59	1.8670	7.61	0.01804	279.01	3.1822	311.91	106.319	344.59	4.3147
287.92	3.2326	99.58	1.9854	12.47	0.09189	287.35	3.2350	311.97	120.733		
301.02	3.4555			13.71	0.1200	294.14	3.2967	312.05	82.050		

$M\{(1/2.80)Cu_{1.80}S\} = 52.303\ g \cdot mol^{-1}$

High-temperature measurements—University of Oslo

Series I		458.18	3.476	656.22	3.505	373.55	3.753	357.08	4.198	Series VII	
301.62	3.478	468.22	3.475	667.04	3.502	378.22	3.721	359.27	4.038	325.39	3.760
311.08	3.683	478.30	3.478	677.88	3.516	Series V		361.50	3.914	327.68	3.798
320.23	3.881	488.43	3.469	688.75	3.534	325.04	4.042	363.77	3.860	329.95	3.838
328.90	4.390	498.62	3.459	699.66	3.534	327.18	4.341	366.05	3.823	332.21	3.882
337.13	4.584	508.83	3.466	710.62	3.547	329.23	4.569	368.35	3.787	334.45	3.911
345.36	4.442	519.09	3.458	Series III		331.23	4.765	370.65	3.744	336.68	4.000
353.48	4.819	529.41	3.453	321.31	3.708	333.20	4.837	372.97	3.734	338.90	4.062
361.89	4.001	539.77	3.442	325.19	3.797	335.16	4.845	Series VI		341.08	4.136
370.94	3.809	550.16	3.436	330.46	3.872	337.11	4.818	345.06	4.265	343.25	4.229

TABLE 2—*continued*

T/K	$C_{p,m}/R$	T/K	$C_{p,m}/R$	T/K	$C_{p,m}/R$	T/K	$C_{p,m}/R$	T/K	$C_{p,m}/R$	T/K	$C_{p,m}/R$
Series II		560.60	3.439	334.96	3.969	339.10	4.651	347.18	4.386	345.39	4.305
380.22	3.710	571.07	3.449	339.39	4.076	341.12	4.545	349.26	4.505	347.50	4.391
389.64	3.658	581.58	3.457	343.72	4.242	343.18	4.397	351.29	4.703	349.58	4.532
399.19	3.591	592.13	3.459	347.95	4.460	345.28	4.335	353.25	5.044	351.61	4.744
408.85	3.559	602.70	3.465	Series IV		347.37	4.406	355.02	6.540	353.56	5.102
418.59	3.531	613.32	3.470	355.75	5.456	349.44	4.558	356.90	4.234	355.34	6.252
428.39	3.512	623.99	3.490	359.82	3.986	351.46	4.775	359.08	4.027	357.26	4.146
438.26	3.489	634.69	3.494	364.33	3.870	353.41	5.103	361.30	3.935	359.45	3.998
448.18	3.487	645.44	3.500	368.91	3.809	355.18	6.400			361.69	3.910
										363.95	3.855
Low-temperature measurements—University of Michigan											
Series VIII		58.66	1.3314	244.90	3.0060	292.33	3.6594	286.92	3.2515	313.90	3.7125
5.26	0.00625	64.91	1.4530	254.87	3.0559	315.09	3.9859	309.99	5.4580	315.89	3.8468
6.03	0.00830	Series IX		264.73	3.0984	336.63	3.8600	321.79	4.7604	317.83	4.0051
7.09	0.01443	52.40	1.2009	274.51	3.1431	342.09	4.8619	336.72	4.8980	319.72	4.0247
8.05	0.02213	57.94	1.3159	284.23	3.2006	Series XIII		341.88	5.2120	321.57	4.2495
9.07	0.03356	63.97	1.4355	294.09	2.2878	282.74	3.1853	347.16	4.9769	323.90	4.4947
10.19	0.05003	69.63	1.5346	303.45	4.1186	285.73	3.2135	Series XVI		326.63	5.0469
11.33	0.06928	76.38	1.6470	308.98	16.510	288.70	3.2564	271.52	3.1429	329.22	5.0319
12.46	0.09153	84.91	1.7873	311.25	17.732	Series XIV		278.89	3.1911	331.78	5.2266
13.66	0.1196	93.88	1.9128	316.61	4.2627	63.36	1.4179	286.15	3.2516	334.65	5.4371
15.01	0.1538	104.00	2.0400	324.78	4.7085	96.06	1.9327	293.24	3.3885	340.19	5.4705
16.51	0.1941	114.39	2.1606	332.98	4.8530	164.36	2.5731	298.79	3.6579	345.24	5.3059
18.18	0.2425	124.24	2.2673	341.63	4.9719	239.52	2.9876	302.41	4.1173	Series XVII	
20.08	0.3009	134.07	2.3629	348.71	4.7196	270.75	3.1252	304.77	4.7403	291.38	3.8127
22.21	0.3680	144.12	2.4502	Series X		279.34	3.1729	306.29	5.6688	296.26	3.5691
24.51	0.4419	154.20	2.5284	298.98	3.4635	287.46	3.2296	307.55	7.2521	301.45	3.4915
27.07	0.5234	164.29	2.5977	320.73	3.5043	304.03	6.1604	308.51	10.165	306.68	3.5475
29.89	0.6120	174.26	2.6598	Series XI		326.79	4.7187	309.23	13.681	311.83	3.6332
32.93	0.7065	184.26	2.7188	275.38	3.1583	338.80	5.0589	309.77	17.554	316.87	3.7074
36.15	0.8008	194.39	2.7735	285.50	3.2411	342.70	5.0457	310.22	20.557	321.85	3.7518
39.83	0.9023	204.46	2.8172	295.59	3.5244	346.67	4.9026	310.62	22.223		
44.15	1.0110	214.58	2.8683	316.79	5.7690	Series XV		311.01	21.697		
48.12	1.1059	224.70	2.9158	Series XII		271.58	3.1400	311.47	16.545		
52.72	1.2084	234.82	2.9600	282.74	3.2951	279.40	3.1886	312.31	6.9433		

$M\{(1/2.85)Cu_{1.85}S\} = 52.500\ g \cdot mol^{-1}$

High-temperature measurements—University of Oslo

Series I		530.06	3.415	Series II		312.00	4.003	356.65	7.154	311.98	5.788
326.07	3.689	540.63	3.417	279.39	3.253	314.17	3.399	Series IV		312.93	3.691
335.29	4.048	551.24	3.421	299.69	3.736	316.43	3.487	301.35	3.678	314.04	3.340
343.86	4.735	561.90	3.421	301.78	4.160	318.66	3.557	304.46	4.400	315.18	3.389
351.40	6.146	572.59	3.424	303.72	4.650	320.85	3.700	306.28	5.418	Series VI	
357.85	7.557	583.32	3.430	305.53	5.257	322.99	3.803	307.54	5.744	297.72	3.250
364.39	5.932	594.10	3.434	307.20	5.848	325.10	3.975	308.32	6.578	298.95	3.270
371.52	5.890	604.90	3.441	308.79	6.194	327.13	4.162	309.04	7.214	300.16	3.456
379.19	4.821	615.76	3.447	310.47	4.842	329.11	4.370	309.71	7.945	301.33	3.588
387.99	3.802	626.64	3.453	312.51	3.457	331.05	4.474	310.33	8.692	302.47	3.763
397.57	3.627	637.57	3.457	314.74	3.462	332.98	4.540	311.00	6.752	303.92	4.246
407.34	3.570	648.55	3.459	316.97	3.530	335.76	4.580	311.82	4.793	305.36	4.801
417.21	3.537	659.58	3.463	319.16	3.625	338.57	4.757	312.83	3.423	306.29	5.320

TABLE 2—*continued*

T/K	$C_{p,m}/R$	T/K	$C_{p,m}/R$	T/K	$C_{p,m}/R$	T/K	$C_{p,m}/R$	T/K	$C_{p,m}/R$	T/K	$C_{p,m}/R$
427.16	3.506	670.67	3.468	321.30	3.861	340.38	4.938	Series V		307.14	5.984
437.18	3.487	681.80	3.460	323.37	3.940	342.20	4.955	299.40	3.421	307.93	6.710
447.27	3.464	692.97	3.476	Series III		343.97	5.337	303.77	4.008	308.66	7.409
457.41	3.470	704.17	3.476	298.80	3.347	345.67	5.428	306.73	5.061	309.35	7.987
467.63	3.451	715.41	3.489	303.19	4.100	347.35	5.593	308.02	5.844	310.04	7.338
477.93	3.431	726.67	3.500	306.12	5.179	349.08	5.648	308.78	7.038	310.82	5.433
488.28	3.428	737.98	3.506	307.75	6.411	350.79	5.901	309.46	7.896	311.80	3.735
498.67	3.425	749.36	3.498	308.88	6.655	352.41	6.174	310.08	8.876	312.93	3.369
509.09	3.421	760.80	3.505	309.57	7.700	353.90	6.851	310.67	9.065	314.10	3.379
519.55	3.419	772.28	3.513	310.26	6.793	355.28	7.036	311.27	8.419		

Low-temperature measurements—University of Michigan

Series VII		263.82	3.0732	13.80	0.1280	Series XI		313.37	3.4375	303.46	4.1991
106.44	2.0501	273.73	3.1209	15.12	0.1622	294.36	3.2627	316.06	3.4657	305.54	5.0797
115.36	2.1533	283.65	3.1786	16.70	0.2061	302.04	3.6306	318.72	3.5465	307.27	6.3561
125.08	2.2555	293.26	3.2659	18.43	0.2582	307.83	6.7305	321.34	3.6090	308.69	7.9941
135.05	2.3527	Series IX		20.40	0.3210	312.37	5.8365	327.63	3.8443	309.89	8.9470
145.26	2.4391	70.28	1.5152	22.95	0.4042	318.45	3.6288	336.71	4.5819	311.29	5.9135
155.35	2.5182	77.24	1.6330	26.04	0.5073	325.31	4.2614	344.33	5.7861	313.44	3.4843
Series VIII		85.18	1.7644	29.31	0.6156	331.43	4.7319	Series XIII		319.80	3.6095
154.56	2.5115	94.75	1.9008	33.81	0.7038	337.03	5.2196	236.25	2.9379	329.31	4.4178
164.13	2.5751	105.68	2.0397	37.20	0.7993	342.27	5.4803	287.98	3.2214	338.24	5.1558
174.15	2.6398	116.59	2.1668	41.37	0.9082	346.69	5.9233	296.40	3.4800	346.20	6.0214
184.08	2.6936	Series X		46.24	1.0276	Series XII		303.68	4.7331	Series XV	
193.84	2.7413	8.43	0.02926	51.36	1.1437	293.47	3.4082	309.83	6.6019	295.51	3.4463
213.91	2.8397	8.98	0.03493	56.74	1.2585	300.57	3.9554	315.22	3.4722	311.68	4.7127
223.71	2.8807	9.81	0.04685	62.54	1.3739	304.89	4.8960	320.31	3.6167	334.35	4.6661
233.71	2.9272	10.65	0.06258	68.76	1.4895	306.75	5.3277	Series XIV			
243.72	2.9730	11.60	0.07934	75.77	1.6089	308.61	5.2173	293.26	3.2659		
253.77	3.0210	12.65	0.1008			310.78	3.8140	298.59	3.5300		

High-temperature measurements—University of Oslo

Series XVI		Series XVII		340.60	4.129	355.99	7.156	370.21	4.282	Series XVIII	
298.87	3.442	300.20	3.256	343.56	4.635	358.81	7.433	371.22	4.330	379.24	4.799
304.06	4.109	303.79	3.296	346.38	4.936	361.61	7.577	372.22	4.462	380.18	4.859
306.88	5.578	307.30	3.342	348.09	5.160	362.30	7.938	373.20	4.643	381.14	4.619
308.26	6.805	310.76	3.403	348.98	5.424	362.96	8.070	374.15	4.907	382.11	4.679
311.84	4.465	314.20	3.446	349.84	5.581	363.62	8.046	375.08	5.052	383.09	4.522
315.02	3.436	317.60	3.517	350.68	5.990	364.29	7.926	375.98	5.052	385.05	4.573
324.56	3.583	320.98	3.565	351.49	6.110	364.97	7.734	376.86	5.412	388.10	4.145
327.82	4.125	324.35	3.606	352.27	6.555	365.67	7.241	377.73	5.761	391.26	4.016
330.92	4.340	327.68	3.646	353.03	6.675	366.41	6.507	378.61	5.015	394.49	3.848
333.87	4.836	330.98	3.721	353.78	6.771	367.24	5.304	379.41	4.715	397.82	3.701
		334.24	3.801	354.53	6.880	368.18	4.414			401.20	3.608
		337.46	3.891	355.27	7.000	369.19	4.234				

TA 3000 system consisting of a TG10 TA processor and a DSC30 cell. Samples of ≈ 50 mg were used, the heating rate was $0.17\ \mathrm{K \cdot s^{-1}}$ and the temperature range ≈ 100 to ≈ 800 K was covered. Reduction of results and evaluation of transition temperatures were performed with standard programs for the system.

3. Results and discussion

HEAT CAPACITY AND THERMODYNAMIC PROPERTIES

The experimental molar heat capacities for (1/2.75)$Cu_{1.75}S$, for (1/2.80)$Cu_{1.80}S$, and for (1/2.85)$Cu_{1.85}S$ over both low- and high-temperature ranges are listed in chronological order for the mean temperatures in table 2, and presented graphically in figure 2. The approximate temperature increments used in the determinations can usually be inferred from the adjacent mean temperatures in table 2.

Twice the standard deviation in the measured low-temperature heat capacity is about 1 per cent from 8 to 30 K, 0.1 per cent from 30 to 300 K, and 0.2 per cent from 300 to 350 K. In the higher-temperature region it is about 0.3 per cent.

The experimental heat capacities for the low- and high-temperature series were fitted to polynomials in temperature by the method of least squares. The fitting and especially the joins between the fitted segments were checked by inspection of plots of $dC_{p,m}/dT$ against T. The polynomials were then integrated, by Simpson's rule,[41] to yield values of thermodynamic functions at selected temperatures, see table 3. Within the transition regions the heat capacities were read from large-scale plots and the thermodynamic functions were calculated by integration of the curves. At the lowest temperatures the heat capacities were smoothed with the aid of plots of $C_{p,m}/T$ against T^2 and the functions evaluated by extrapolation of this function. From this plot γ was found to be zero within experimental error limits for all three samples.

In all three samples a pronounced endothermic effect with origin in a structural phase transition from anilite to low-digenite was observed around 312 K. The nature of the transition was confirmed by powder X-ray diffraction. The X-ray photographs of the samples which had been held at 290 K for more than 2 a showed, as earlier reported,[30] the presence of anilite, but with somewhat diffuse lines due to hysteresis in the attainment of equilibrium. After refrigeration at 275 K for 15 h, Guinier photographs produced sharp lines. The transition temperature of the first-order transition, is around 268 K on cooling as detected by d.t.a. The X-ray powder results obtained for anilite are given in table 4, while the derived lattice constants, as well as those of Morimoto *et al.*[19] and of Potter and Evans,[33] are listed in table 1. Powder X-ray diffraction shows two transitions, one around 312 K, where anilite transforms to low-digenite, and an additional one around 353 K, where low-digenite transforms to high-digenite. The X-ray powder results obtained for quenched 5*a* and 6*a*-types of low-digenite, as well as lattice constants for high-digenite, are given in table 4, together with results by previous investigators. The earlier investigations of the anilite/digenite region contain many contradictory observations. These may partly originate from the low transition temperature of anilite, and partly from the fact that anilite transforms to low-digenite on grinding. In addition, the large hysteresis requires the last step in the synthesis of anilite to be cooling below 268 K. In previous investigations two stability limits have been proposed. Potter[28] and Morimoto and Koto[20] reported an upper stability limit for anilite around 345 K, while Gezalov *et al.*[31] reported the anilite-to-low-digenite transition to occur around 312 K, in agreement with our observations. (The reason

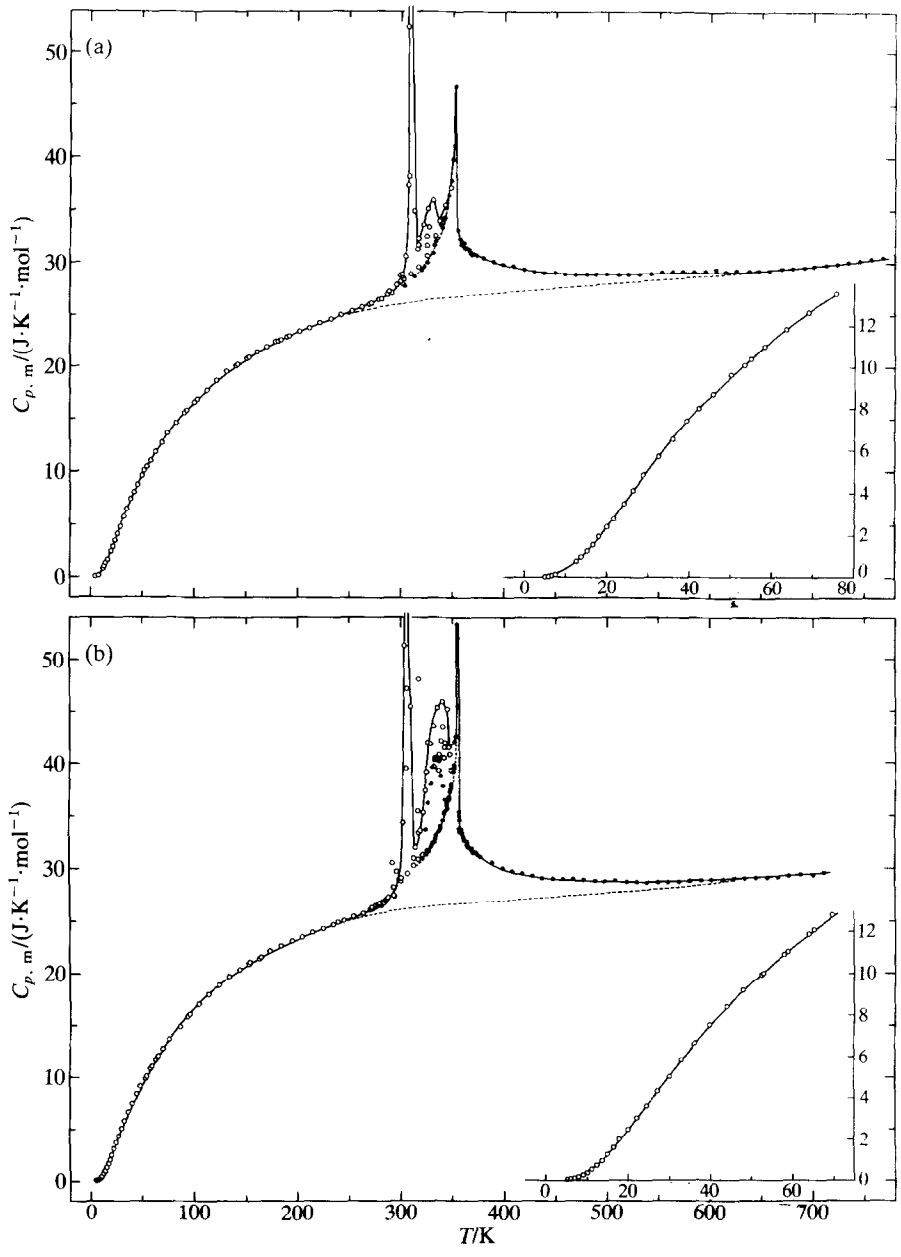

why Potter[28] did not observe this transition, might be that only three measurements were made below the transition temperature, see figure 7 in his paper.)

Results of the transformation evaluations are given in table 5. The estimated lattice heat capacity at constant pressure was derived by extrapolating the constant-

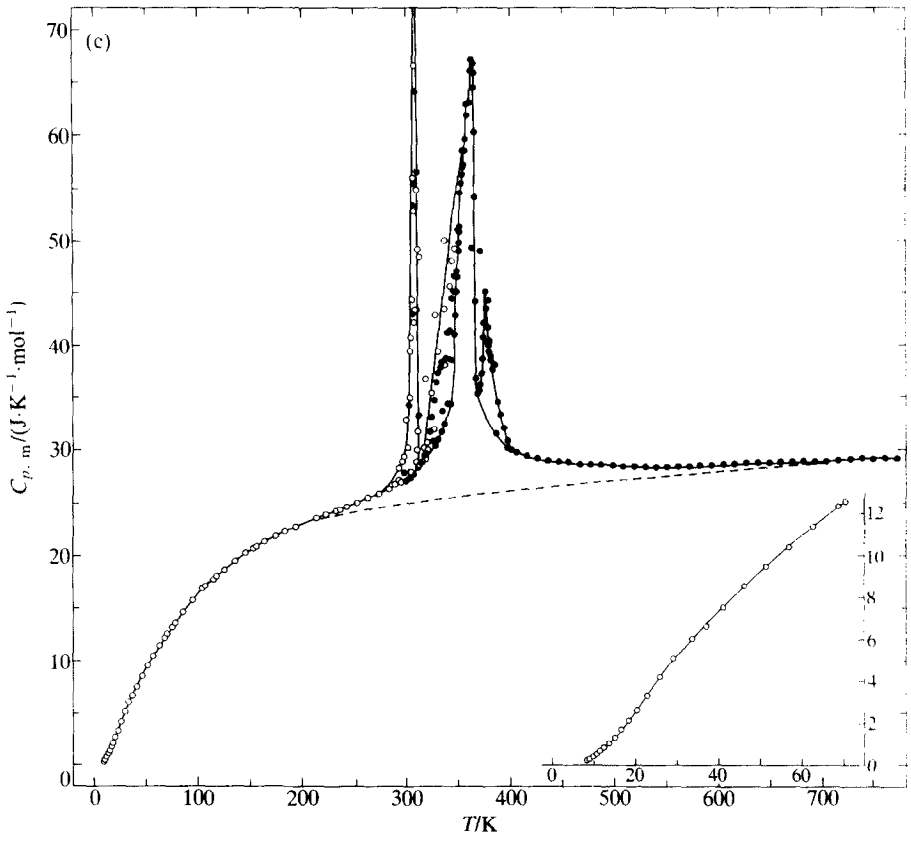

FIGURE 2. Molar heat capacity (a), of (1/2.75)$Cu_{1.75}S$; (b), of (1/2.80)$Cu_{1.80}S$, and (c), of (1/2.85)$Cu_{1.85}S$. ●, Low-temperature measurements (University of Michigan); ○, high-temperature measurements (University of Oslo); – – –, estimated lattice contribution: $C_{V,m} + C_m(d)$.

volume heat capacity in the harmonic approximation—using a constant Debye temperature—into the higher-temperature region, and adding a dilational heat-capacity term.

The constant Debye temperature was taken as the maximum of Θ_D in a plot of Θ_D against temperature. It turned out to be 315 K for $Cu_{1.75}S$, and 314 K for $Cu_{1.80}S$ and $Cu_{1.85}S$. The dilational heat capacity was derived according to Nernst and Lindemann[42] as

$$C_m(d) = AC_{p,m}^2 T_f/T,$$

where $A = 6.1 \times 10^{-4} R^{-1}$ was considered to be a universal constant and T_f denotes the melting temperature. In the present investigation the constant A was determined under the condition that $C_{V,m}(\text{lattice}) + C_m(d) = C_{m,\text{expt}}$ in the high-temperature region ($T > 600$ K) for all three samples. The observed values of A and T_f[22] respectively for $Cu_{1.75}S$, $Cu_{1.80}S$, and $Cu_{1.85}S$ are $1.09 \times 10^{-3} R^{-1}$, 1050 K; $1.11 \times 10^{-3} R^{-1}$, 1210 K; $1.07 \times 10^{-3} R^{-1}$, 1290 K. These correspond to $\Gamma = 2.33$,

TABLE 3. Thermodynamic properties ($R = 8.3144\ \mathrm{J \cdot K^{-1} \cdot mol^{-1}}$)

T/K	$C_{p,m}/R$	$\Delta_0^T S_m^\circ(T)/R$	$\Delta_0^T H_m^\circ(T)/R \cdot \mathrm{K}$	$\Phi_m^\circ(T,0)/R$	T/K	$C_{p,m}/R$	$\Delta_0^T S_m^\circ(T)/R$	$\Delta_0^T H_m^\circ(T)/R \cdot \mathrm{K}$	$\Phi_m^\circ(T,0)/R$
			$M\{(1/2.75)Cu_{1.75}S\} = 52.099\ \mathrm{g \cdot mol^{-1}}$						
0	0	0	0	0	280	3.187	4.498	590.21	2.390
10	0.0462	0.0137	0.1050	0.00320	298.15	3.354	4.702	649.2	2.526
15	0.1523	0.0506	0.5779	0.01207	300	3.368	4.722	655.4	2.538
20	0.2976	0.1137	1.6924	0.02908	320	3.947	5.251	819.9	2.689
25	0.4574	0.1971	3.5768	0.05403	330	4.276	5.380	861.8	2.769
30	0.6180	0.2949	6.271	0.08587	340	4.005	5.504	903.6	2.846
40	0.9020	0.5126	13.906	0.1650	350	4.931	5.631	947.0	2.925
50	1.1479	0.7410	24.188	0.2573	360	3.807	5.756	991.1	3.003
60	1.3557	0.9693	36.734	0.3570	370	3.714	5.860	1028.6	3.079
70	1.5369	1.192	51.212	0.4604	380	3.653	5.957	1065.4	3.154
80	1.7043	1.408	67.425	0.5655	400	3.575	6.142	1137.7	3.298
90	1.858	1.618	85.250	0.6709	420	3.522	6.316	1208.5	3.439
100	1.993	1.821	104.53	0.7758	440	3.490	6.479	1278.5	3.573
120	2.217	2.205	146.69	0.9824	460	3.480	6.634	1347.1	3.706
140	2.414	2.562	193.04	1.1828	500	3.478	6.924	1487.4	3.950
160	2.571	2.895	242.98	1.3762	550	3.488	7.256	1661.6	4.235
180	2.693	3.205	295.64	1.5624	600	3.502	7.560	1836.3	4.500
200	2.808	3.495	350.67	1.742	650	3.528	7.842	2011.9	4.746
220	2.901	3.767	407.82	1.914	700	3.571	8.104	2189.3	4.977
240	2.998	4.023	466.70	2.078	750	3.638	8.353	2369.5	5.193
260	3.079	4.266	527.46	2.238					
			$M\{(1/2.80)Cu_{1.80}S\} = 52.303\ \mathrm{g \cdot mol^{-1}}$						
0	0	0	0	0	260	3.075	4.269	527.23	2.241
10	0.0467	0.0140	0.1073	0.00327	280	3.187	4.499	589.76	2.393
15	0.1531	0.0511	0.5831	0.01227	298.15	3.614	4.708	650.2	2.527
20	0.2983	0.1145	1.7015	0.02935	300	3.692	4.730	656.6	2.541
25	0.4569	0.1980	3.5890	0.05448	320	4.378	5.193	800.5	2.692
30	0.6162	0.2954	6.2702	0.0864	330	4.931	5.340	848.2	2.770
40	0.9060	0.5137	13.930	0.1655	340	5.208	5.498	900.5	2.849
50	1.1479	0.7426	24.229	0.2580	350	4.979	5.646	951.7	2.926
60	1.3589	0.9710	36.788	0.3578	360	3.975	5.788	1000.8	3.008
70	1.5418	1.1944	51.311	0.4614	370	3.771	5.893	1039.3	3.085
80	1.7072	1.4113	67.57	0.5666	380	3.702	5.993	1076.7	3.160
90	1.859	1.6213	85.41	0.6722	400	3.608	6.181	1149.8	3.306
100	1.994	1.825	104.70	0.7773	420	3.513	6.354	1220.9	3.447
120	2.219	2.208	146.89	0.9842	440	3.507	6.516	1291.0	3.582
140	2.419	2.565	193.33	1.1849	460	3.487	6.672	1360.9	3.713
160	2.568	2.899	243.27	1.3787	500	3.453	6.960	1499.7	3.961
180	2.694	3.209	295.90	1.5650	550	3.448	7.289	1672.0	4.248
200	2.801	3.499	350.91	1.7440	600	3.468	7.590	1844.9	4.516
220	2.889	3.769	407.80	1.916	650	3.495	7.868	2018.8	4.763
240	2.989	4.026	466.56	2.081	700	3.541	8.129	2194.8	4.994
			$M\{(1/2.85)Cu_{1.85}S\} = 52.500\ \mathrm{g \cdot mol^{-1}}$						
0	0	0	0	0	260	3.053	4.220	521.47	2.2144
10	0.0504	0.0167	0.1231	0.00440	280	3.157	4.449	583.55	2.365
15	0.1585	0.0561	0.6253	0.01441	298.15	3.246	4.650	641.82	2.497
20	0.3084	0.1214	1.7792	0.03244	300	3.259	4.671	647.83	2.512
25	0.4668	0.2075	3.7245	0.05852	320	3.668	4.989	746.22	2.657
30	0.6051	0.3044	6.392	0.09133	340	5.441	5.259	835.46	2.802

TABLE 3—*continued*

T/K	$C_{p,m}/R$	$\Delta_0^T S_m^\circ(T)/R$	$\Delta_0^T H_m^\circ(T)/R\cdot K$	$\Phi_m^\circ(T,0)/R$	T/K	$C_{p,m}/R$	$\Delta_0^T S_m^\circ(T)/R$	$\Delta_0^T H_m^\circ(T)/R\cdot K$	$\Phi_m^\circ(T,0)/R$
40	0.8723	0.5157	13.802	0.1707	350	6.495	5.432	895.23	2.874
50	1.1111	0.7366	26.148	0.2136	360	7.495	5.629	965.11	2.948
60	1.3235	0.9584	35.937	0.3595	370	4.257	5.813	1031.2	3.026
70	1.5122	1.1768	50.133	0.4606	380	4.750	5.942	1080.1	3.100
80	1.6808	1.3899	66.114	0.5635	400	3.625	6.151	1162.0	3.246
90	1.832	1.5968	83.692	0.6669	420	3.520	6.324	1232.8	3.389
100	1.969	1.797	102.71	0.7699	440	3.488	6.487	1303.0	3.526
120	2.203	2.177	144.51	0.9728	460	3.456	6.641	1372.4	3.658
140	2.396	2.532	190.58	1.1707	500	3.422	6.928	1509.8	3.908
160	2.550	2.863	240.09	1.3624	550	3.417	7.254	1680.7	4.198
180	2.671	3.170	292.34	1.5459	600	3.437	7.552	1852.0	4.465
200	2.772	3.457	346.81	1.7230	650	3.462	7.828	2024.5	4.713
220	2.865	3.725	403.20	1.8923	700	3.476	8.085	2198.0	4.945
240	2.956	3.979	461.40	2.0565	750	3.508	8.326	2372.6	5.163

1.91, and 1.66 for $Cu_{1.75}S$, $Cu_{1.80}S$, and $Cu_{1.85}S$, respectively, where Γ is a parameter in the Grüneisen approximation:[43] $C_m(d) = \alpha\Gamma C_{V,m}T$. Here $\alpha = 1.4\times10^{-4}\,K^{-1}$ was used in the range 273 to 773 K for all three samples. The estimated lattice heat capacities and the allocation of the transitional enthalpy to the different transitions are presented in figure 2. Pre-transitional heat-capacity values for low-digenite (plus covellite or djurleite) are used as reference for the anilite-to-low-digenite transition for the three copper sulfides, as well as for the phase reactions occurring below 355 K. The evaluations show unusually large spread, with low values for incompletely transformed samples due to insufficient cooling or short equilibration times at the most suitable temperatures; see table 6 for thermal history. Some results for $Cu_{1.85}S$ are shown in figure 3.

For each composition the highest values for the transition were taken to represent complete equilibration. They are for the anilite-to-low-digenite transition:

$$(1/2.75)Cu_{1.75}S:\quad \Delta_{trs}H_m^\circ = 94.80R\cdot K;\quad \Delta_{trs}S_m^\circ = 0.304R.$$
$$(1/2.80)Cu_{1.80}S:\quad \Delta_{trs}H_m^\circ = 72.49R\cdot K;\quad \Delta_{trs}S_m^\circ = 0.233R.$$
$$(1/2.85)Cu_{1.85}S:\quad \Delta_{trs}H_m^\circ = 31.28R\cdot K;\quad \Delta_{trs}S_m^\circ = 0.101R.$$

The pre-transitional component of the transition is not included in this approximate resolution of the anilite-to-low-digenite component, but comes in as a part of the low-to-high-digenite transition.

On the basis of the Cu-rich composition limit of djurleite reported by Potter,[28] $Cu_{1.934}S$, and the value of the transitional enthalpy of anilite, $Cu_{1.75}S$, the expected values for $\Delta_{trs}H_m^\circ$ for $Cu_{1.80}S$ and $Cu_{1.85}S$ are $68.9R\cdot K$ and $39.8R\cdot K$, respectively. They are in reasonable agreement with the experimental values and substantiate the compositional values for anilite and djurleite.

The structural phase transition from low-digenite to high-digenite is observed as a peak in the heat-capacity curve around 353 K in both $Cu_{1.75}S$ and $Cu_{1.80}S$, and as

TABLE 4. X-ray powder results characterizing the observed phases (Cu Kα_1 radiation)

I(obs)	*hkl*	$10^5(\sin\theta)^2$	*I*(calc)	*I*(obs)	*hkl*	$10^5(\sin\theta)^2$	*I*(calc)
			Anilite ($Cu_{1.75}S$) at 295 K				
vw	101	1430	68	s	124	12640	423
w	112	3858	119	m	321	12930	164
s	211	5252	396	m	033	13105	202
s	121	5294	221	m	313	13918	80
m	103	5346	181	s	133	14055	213
vs	202	5755	392	s	400	15202	214
m	022	5816	135	vs	224	15470	1000
w	113	6305	28	m	401	15722	155
w	212	6707	10	w	205	16050	41
vs	220	7669	413	m	304	16395	138
m	004	7829	141	m	323	16791	100
s	221	8167	344	m	125	17061	36
s	104	8777	241	m	314	17370	67
vw	301	9042	28	m	142	18365	104
s	031	9175	260	w	240	19244	50
w	311	10019	77	m	403	19674	86
vw	131	10134	28	m	422	21058	186
s	302	10533	190	m	242	21199	185
vw	204	11603	1	m	026	21482	125
m	223	12065	171				

I(obs)	$h^2+k^2+l^2$	$10^5(\sin\theta)^2$	*I*(obs)	$h^2+k^2+l^2$	$10^5(\sin\theta)^2$
		Quenched 5*a*-type low-digenite ($Cu_{1.75}S$) at 295 K, $a = (2773 \pm 1)$ pm			
vw	67	5142	vs	201	15462
vw	68	5247	vw	227	17520
vw	72	5560	w	243	18742
vs	75	5807	vw	248	19101
m	83	6406	vw	267	20592
s	100	7718	vs	275	21207
vw	107	8235	vw	280	21746
vw	123	9465	w	299	23099
vw	132	10150	vw	360	27943
vw	152	11687	w	400	30842
w	163	12576	vw	408	31416
		Quenched 6*a*-type low-digenite ($Cu_{1.80}S$) at 295 K, $a = (3340 \pm 1)$ pm			
vw	99	5253	vw	339	18027
s	108	5790	vw	360	19058
w	123	6545	vw	363	19281
vs	144	7676	s	396	21096
vw	196	10369	vw	411	21823
vw	204	10849	vw	432	22977
vw	243	12936	vw	459	24379
vs	288	15285	vw	528	28184
vw	291	15428	vw	576	30679
vw	336	17810			

TABLE 4—*continued*

T/K	a/pm		
	$Cu_{1.75}S$	$Cu_{1.80}S$	$Cu_{1.85}S$
	Unit-cell parameters of high-digenite: Present results		
323	556.1±0.2	557.1±0.2	
353	556.5±0.2	557.7±0.2	
388	556.9±0.2	558.1±0.2	559.3±0.2
423	557.1±0.2	558.4±0.2	560.0±0.2
453	557.7±0.3	558.6±0.2	560.4±0.2
523	559.0±0.3	559.5±0.2	561.2±0.2
	Previous investigations at T = 473K:		

$Cu_{1.69}S$, 557.8;[14] $Cu_{1.77}S$, 557.8;[14] $Cu_{1.79}S$, 558.7;[14] $Cu_{1.80}S$, 560;[34] $Cu_{1.84}S$, 561.0;[14] $Cu_{1.90}S$, 536.7[14]

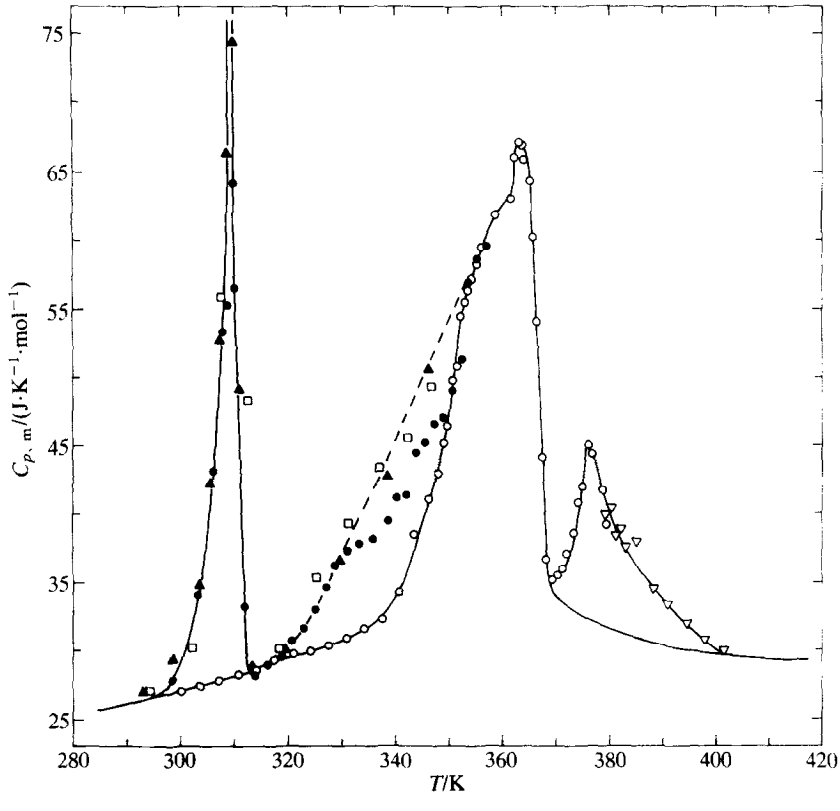

FIGURE 3. Effect of thermal history on the heat capacity of $Cu_{1.85}S$: ●, Series III (after 4 d at 250 K); □, Series XI (heated from 80 K); ▲, Series XIV (cooled to 183 K, then heated to 290 K); ○, Series XVII (after exploratory runs to 373 K); ▽, Series XVIII (after 14 d at 358 K).

TABLE 5. Enthalpies and entropies of transition ($R = 8.3144\ J \cdot K^{-1} \cdot mol^{-1}$)

Series	Detn.	$\Delta_m H_{exc}/R \cdot K$	$\Delta_m S_{exc}/R$	Series	Detn.	$\Delta_m H_{exc}/R \cdot K$	$\Delta_m S_{exc}/R$	Series	Detn.	$\Delta_m H_{exc}/R \cdot K$	$\Delta_m S_{exc}/R$
					$M\{(1/2.75)Cu_{1.75}S\} = 52.099\ g \cdot mol^{-1}$						
Anilite to low-digenite transition: $T_{trs} = 312.0$ K											
IV	13 to 17	94.80	0.304	VI	1 to 2	88.52	0.284	XIII	3 to 18	87.52	0.280
V	1 to 3	90.98	0.291	VII	2 to 4	88.67	0.284	XIV	1 to 3	1.48	0.0048
Phase reaction (315 to 350 K)											
XIII	19 to 26	12.03	0.035								
Low-digenite to high-digenite transition (250 to 650 K)											
	Smoothed $C_{p,m}$s									89.00	0.237
					$M\{(1/2.80)Cu_{1.80}S\} = 52.303\ g \cdot mol^{-1}$						
Anilite to low-digenite transition: $T_{trs} = 311.0$ K											
IX	26 to 31	72.49	0.233	XIV	7 to 8	63.78	0.206	XVII	1 to 5	5.94	0.019
X	1 to 2	34.75	0.112	XV	3 to 4	69.77	0.225				
XI	2 to 3	12.12	0.039	XVI	3 to 18	63.87	0.206				
Phase reaction (315 to 350 K)											
V	1 to 13	12.28	0.036	XII	4 to 5	19.67	0.059	XV	5 to 8	8.80	0.027
IX	32 to 35	30.93	0.093	XIV	9 to 12	33.36	0.101	XVI	19 to 29	27.54	0.083
Low-digenite to high-digenite transition (250 to 650 K)											
	Smoothed $C_{p,m}$s									108.5	0.29
					$M\{(1/2.85)Cu_{1.85}S\} = 52.500\ g \cdot mol^{-1}$						
Anilite to low-digenite transition: $T_{trs} = 309.5$ K											
II	1 to 10	20.99	0.067	VI	1 to 16	22.47	0.072	XIV	1 to 9	28.04	0.090
III	1 to 9	20.60	0.066	XI	1 to 4	30.14	0.097	XVI	1 to 5	21.35	0.069
IV	1 to 11	25.11	0.081	XII	1 to 7	18.25	0.059	XVII	1 to 5	1.00	0.0036
V	1 to 12	27.01	0.088	XIII	3 to 6	31.28	0.101				
Phase reaction (320 to 350 K)											
III	9 to 30	19.16	0.058	XII	8 to 13	18.92	0.057				
XI	5 to 10	30.72	0.091	XIV	10 to 13	26.83	0.079				
	Smoothed $C_{p,m}$s (broken curve, figure 3)									30.41	0.089
Low-digenite to high-digenite + djurleite transition (220 to 670 K)											
	Smoothed $C_{p,m}$s									180.58	0.653
Phase reaction (365 to 400 K)											
	Smoothed $C_{p,m}$s									15.92	0.042

a shoulder on the peak around 368 K in $Cu_{1.85}S$. This peak originates from the transition of djurleite to high-digenite and low-chalcocite. The higher-temperature transition in $Cu_{1.85}S$ results from a phase reaction which gives high-digenite as the high-temperature phase.

In addition to contributions from structural phase transitions, heat-capacity effects with origins in phase reactions are observed. The enthalpies of the phase

TABLE 6. Thermal history

Series	Previous treatment	Series	Previous treatment
$Cu_{1.75}S$			
I	Cooled from 670 K to room temperature with furnace	VIII	Cooled to 50 K (70 h)
II	Cooled to room temperature	IX	Cooled to 70 K (6 h), then heated to 135 K (4 h)
III	Cooled overnight	X	Cooled to 88 K (24 h)
IV	Cooled to 178 K after 3 a at room temperature	XI	Cooled to 4.5 K (32 h)
V	Cooled overnight to 240 K	XII	Enthalpy runs from 56 to 266 K
VI	Cooled overnight to 220 K	XIII	Cooled to 160 K (5 d)
VII	Cooled to 180 K (50 h)	XIV	Cooled to 293 K (10 h)
$Cu_{1.80}S$			
I	Cooled from 670 K to room temperature with furnace	IX	Cooled from 70 to 50 K overnight
II	Held at 375 K overnight	X	Cooled from 350 to 290 K (8 h)
III	Cooled overnight	XI	Cooled to 270 K (17 h)
IV	Held at 350 K overnight	XII	Cooled to 278 K (48 h)
V	After 1.25 a at room temperature	XIII	Cooled to 175 K (15 h)
VI	Cooled overnight	XIV	Cooled to 50 K (26 h), 4 enthalpy runs (63 to 267 K)
VII	Cooled to room temperature with furnace	XV	Cooled to <115 K (24 h), heated to 268 K
VIII	2 a at room temperature, then cooled to 5 K before start	XVI	Cooled to 90 K (24 h), heated to 268 K
		XVII	Cooled to 290 K (40 min)
$Cu_{1.85}S$			
I	Cooled from 670 K to room temperature with furnace	XI	Heated from 80 to 290 K
II	After 3 a at room temperature	XII	Cooled to 264 K (11 h), then heated to 290 K
III	After 4 d at 250 K	XIII	Cooled to 183 K (20 h), enthalpy runs (189 to 283 K)
IV	After 3 d at 250 K	XIV	Cooled to 120 K (18 h), then heated to 290 K
V	After 18 h at 230 K	XV	Cooled to 157 K (11 h), then heated to 290 K
VI	After 60 d at 340 K, 2 d at 230 K, and 60 d at room temperature	XVI	After 30 d at room temperature
VII	Cooled to 100 K after 4 a at room temperature	XVII	After exploratory runs to 373 K
VIII	Cooled to 150 K	XVIII	After 14 d at 358 K
IX	Cooled to 65 K (14 h)		
X	Cooled to 8 K (50 h)		

reactions in $Cu_{1.75}S$ and $Cu_{1.80}S$ indicate that the composition limits of low-digenite change with temperature. It appears from the values (see table 5) that the change in the copper-rich phase limit is about three times the shift in the sulfur-rich phase limit. These observations are in contrast to the results of Potter[28] where the compositional limits of low-digenite were found to change much more with temperature on the copper-rich side. In addition the phase diagram proposed by Potter[28] implies that low-digenite with composition $Cu_{1.80}S$ is stable relative to {low-digenite ($Cu_{\approx 1.78}S$) + djurleite} at 310 K. Hence, we should not have observed any phase reactions in the $Cu_{1.80}S$ sample. The composition limits of the low-digenite field indicated in figure 2 are shifted to values consistent with the observed enthalpies of the phase reactions. Moreover, the presently obtained stability limit of anilite is taken into consideration. In $Cu_{1.85}S$ the phase reaction

manifests itself as a contribution on the low-temperature side of the more prominent djurleite transition. The phase relations in the region $Cu_{1.90}S$ to $Cu_{2.00}S$ will be treated in a forthcoming paper in this series.

TRANSITIONS

The crystal structures of the observed phases have been the object of a great number of investigations. In spite of this, neither the high-digenite nor the low-digenite structures are fully understood. The proposed models of the structures imply different degrees of positional disorder, hence they may be compared with the observed entropies of the anilite/djurleite-to-low-digenite and the low-digenite-to-high-digenite transitions in so far as they are of configurational origin. It is generally assumed that the two low-temperature phases, anilite and djurleite, are completely ordered.[21,35] Barth[44] originally suggested an antifluorite-type structure for the high-temperature phase with composition Cu_2S. This would give rise to a small positional entropy increment for the transition to high-digenite for a phase with composition $Cu_{2-x}S$. Ralfs[45] examined 19 structural models for digenite, including the anti-fluorite-like structure, without obtaining satisfactory agreement between observed and calculated X-ray intensities. Morimoto and Kullerud[8] found that the intensities obtained by X-ray precession photographs of natural high-digenite were reasonably well explained by a model in which S atoms occupy nodes of the cubic face-centered lattice and each tetrahedron contains 9/10 of a Cu atom randomly distributed over 24 equivalent positions. The structure was interpreted in terms of stacking of S and Cu layers along [111], (. . . CuSCuSCuSCuSCu . . .) where CuSCu was considered to be the unit. Their model of low-digenite is based on the structure of the metastable form, in which one Cu layer is removed from every fifth CuSCu unit. In this structure each S tetrahedron contains 1.0 Cu atom randomly distributed over four equivalent positions. The low-temperature form was assumed to result from ordering of the metastable form with preferential occupation of some of the four equivalent positions. A transition from the low-temperature anilite/djurleite phases to metastable low-digenite will then result in a configurational entropy change:

$$\Delta_{\text{conf}}S_{\text{m}} = -7.2R\{(1/4)\ln(1/4)+(3/4)\ln(3/4)\},$$

for $Cu_{1.80}S$. The configurational entropy of the transition from anilite/djurleite to stable low-digenite will on the assumption of preferential occupation of some of the four positions in low-digenite be lower. The resulting value for $(1/2.80)Cu_{1.80}S$ is $1.45R$ while the observed value is only $0.233R$.

Since the heat capacity of (low-digenite + djurleite) is used as background for $Cu_{1.80}S$, the actual entropy of the transition is slightly underestimated. Moreover, the reference lattice heat capacity for $(1/2.80)Cu_{1.80}S$ is somewhat higher than that used earlier for $(1/3)Cu_2S$, which also contributes to the smallness of the estimated transitional entropy. Even so, the discrepancy is rather substantial and indicates that the order-disorder pattern is more complex. Presumably it involves the formation of extended defects.

A transition from metastable low-digenite to high-digenite will result in a configurational entropy change:

$$\Delta_{conf}S_m = -48R\{(0.9/24)\ln(0.9/24) + (23.1/24)\ln(23.1/24)\} + 7.2R\{(1/4)\ln(1/4) + (3/4)\ln(3/4)\},$$

for $Cu_{1.80}S$. The first part of the expression represents the configurational-entropy decrement for a transition from high-digenite to that of an ordered structure, whereas the last part represents the entropy increment for a transition from an ordered structure to metastable low-digenite. The configurational entropy of the transition from stable low-digenite to high-digenite will, on the assumption of preferential occupation of some of the four positions in low digenite, be higher. The resulting value for $(1/2.80)Cu_{1.80}S$ is $1.30R$, while the observed value is $0.29R$. Again, the small transitional entropy indicates the persistence of extended defects.

Kazinets[46] found best agreement between calculated and observed electron-diffraction intensities for the space group F43m with 3.2 Cu atoms in octahedral spaces and 4 Cu atoms at the centers of the 4 S tetrahedra. Gasymov *et al.*[47] placed approximately half of the Cu atoms in 8(c) positions with coordinates (1/3, 1/3, 1/3) and the remaining in 32(f) positions with coordinates (1/4 1/4, 1/4).

Other models based on electron-diffraction investigations show that the distribution of vacancies most probably is more complex.[15-17] This means that models based on the assumption of randomly distributed vacancies are bound to fail, partly because every Cu atom may block a number of sites for occupancy by another Cu, and partly because the non-stoichiometry may be due to formation of vacancy pairs or complexes. Van Dyck *et al.*[16] have derived the structure of digenite by means of cluster theory.[48] They concluded that Cu atoms preferentially occupy infinite (111) layers of tetrahedral sites in high-digenite. Lowering the temperature causes an ordered succession of these planes which gives rise to the observed superstructures. However, such ordering would lead to a smaller configurational entropy change than observed.

The portion of this work done at the University of Michigan was supported by the Structural Chemistry and Chemical Thermodynamics Program, Division of Chemistry, National Science Foundation under Grant No. CHE-7710049, while the work at the University of Oslo was supported by the Norwegian Research Council for Science and the Humanities. The assistance of Bjørn Lyng Nielsen with the preparation of the samples and in the higher-temperature calorimetric measurements and the cooperation of Laurel A. Harmon in the calculation of the thermophysical properties is gratefully acknowledged.

REFERENCES

1. Grønvold, F.; Westrum, E. F., Jr. *J. Chem. Thermodynamics* **1987,** 19, 1183.
2. Westrum, E. F., Jr.; Stølen, S.; Grønvold, F. *J. Chem. Thermodynamics* **1987,** 19, 1199.
3. Buerger, N. W. *Econ. Geol.* **1941,** 36, 19.
4. Buerger, N. W. *Am. Mineral.* **1942,** 27, 712.
5. Wagner, J. B.; Wagner, C. *J. Chem. Phys.* **1957,** 26, 1602.

6. Wehefritz, V. *Z. Phys. Chem. N.F.* **1960,** 26, 339.
7. Rau, H. *J. Phys. Chem. Solids* **1967,** 28, 903.
8. Rau, H. *J. Phys. Chem. Solids* **1974,** 35, 1415.
9. Nagamori, M. *Metall. Trans. B* **1976,** 7, 67.
10. Peronne, R.; Balesdent, D.; Rilling, J. *Bull. Soc. Chim. Fr.* **1972,** 457.
11. Donnay, G.; Donnay, J. D. H.; Kullerud, G. *Am. Mineral.* **1958,** 43, 228.
12. Kullerud, G. *Ann. Rept. U.S. Geophys. Lab. Papers* 1265 (**1955/56**), 1289 (**1957/58**), 1340 (**1959/60**).
13. Morimoto, N.; Kullerud, G. *Am. Mineral.* **1963,** 48, 110.
14. Roseboom, E. H., Jr. *Econ. Geol.* **1966,** 61, 641.
15. Pierce, L.; Buseck, P. R. *Am. Mineral.* **1978,** 63, 1.
16. Van Dyck, D.; Conde-Amiano, C.; Amelinckx, S. *Phys. Stat. Sol. (a)* **1980,** 58, 451.
17. Conde, C.; Monolikas, C.; Van Dyck, D.; Delavignette, P.; Van Landuyt, J.; Amelinckx, S. *Mat. Res. Bull.* **1978,** 13, 1055.
18. Putnis, A. *Am. Mineral.* **1977,** 62, 107.
19. Morimoto, N.; Koto, K.; Shimazaki, Y. *Am. Mineral.* **1969,** 54, 1256.
20. Morimoto, N.; Koto, K. *Am. Mineral.* **1970,** 55, 106.
21. Koto, K.; Morimoto, N. *Acta Cryst.* **1970,** B26, 915.
22. Cook, R. W., Jr. *U.S. Natl. Bur. Stand. Spec. Publ. No. 364,* **1972,** 703.
23. Rickard, D. T. *Tschermaks Mineral. Petrogr. Mitt.* **1973,** 19, 60.
24. Mathieu, H. J.; Rickert, H. *Z. Phys. Chem. N.F.* **1972,** 79, 315.
25. Luquet, H.; Guastavino, F.; Bugnot, J.; Vaissière, J. C. *Mat. Res. Bull.* **1972,** 7, 955.
26. Barton, P. B., Jr. *Econ. Geol.* **1973,** 68, 455.
27. Snellgrove, R. A.; Barness, H. L. *Trans. Am. Geophys. Union* **1974,** 55, 484.
28. Potter, R. W. *Econ. Geol.* **1977,** 72, 1524.
29. Gray, J. N. Dissertation, University of Michigan. **1985.**
30. Grønvold, F., Westrum, E. F., Jr. *Am. Mineral.* **1980,** 65, 574.
31. Gezalov, M. A.; Gasymov, G. B.; Asadov, Yu. G.; Guseinov, G. G.; Belov, N. V. *Sov. Phys. Crystallogr.* **1979,** 24, 700.
32. Gray, J. N.; Clarke, R. *Phys. Rev. B* **1986,** 33, 2056.
33. Potter, R. W.; Evans, H. T., Jr. *J. Research U.S. Geol. Survey* **1976,** 4, 205.
34. Djurle, S. *Acta Chem. Scand.* **1958,** 12, 1415.
35. Takeda, H.; Donnay, J. D. H.; Roseboom, E. H.; Appleman, D. E. *Z. Krist.* **1967,** 125, 404.
36. Westrum, E. F., Jr.; Furukawa, G. T.; McCullough, J. P. *Experimental Thermodynamics, Vol. I.* McCullough, J. P.; Scott, D. W.: Editors. Butterworths: London. **1968,** p. 133.
37. Grønvold, F. *Acta Chem. Scand.* **1967,** 21, 1695.
38. Deslatters, R. D.; Henins, A. *Phys. Rev. Lett.* **1973,** 31, 972.
39. Ersson, N. O. Personal communication.
40. Yvon, K.; Jeitschko, W.; Parthé, E. *J. Appl. Crystallogr.* **1977,** 10, 73.
41. Apostol, T. M. *Calculus, Vol. II.* Wiley: New York. **1969,** p. 608.
42. Nernst, W.; Lindemann, F. A. *Z. Elektrochem.* **1911,** 17, 817.
43. Grüneisen, E. *Handbuch der Physik.* Springer Verlag: Berlin. **1926,** Vol. 10, p. 1.
44. Barth, T. *Zentralbl. Mineral. Geol. Paläont. A* **1926,** 284.
45. Rahlfs, P. *Z. Phys. Chem. B* **1936,** 31, 157.
46. Kazinets, M. M. *Sov. Phys. Crystallogr.* **1970,** 14, 599.
47. Gasymov, G. B.; Asadov, Yu. G.; Guseinov, G. G.; Gezalov, M. A.; Belov, N. V. *Dokl. Akad. Nauk SSSR* **1978,** 239, 846.
48. Van Dyck, D.; Conde, C.; Amelinckx, S. *Phys. Stat. Sol. (a)* **1979,** 56, 327.